

BJP

Bangladesh Journal of Pharmacology

Research Article

Ginkgolide B alleviates renal and podocyte injury in membranous nephropathy by inhibiting ferroptosis

Ginkgolide B alleviates renal and podocyte injury in membranous nephropathy by inhibiting ferroptosis

Daoyuan Lv, Yuqing Su, Jun Li, Huixian Zhu, Qiong Tang, and Yafen Yu

Department of Nephrology, Affiliated Hospital of Jiangnan University, Wuxi 214122, China.

Article Info

Received: 19 July 2025
 Accepted: 29 August 2025
 Available Online: 31 August 2025
 DOI: 10.3329/bjp.v20i3.83064

Cite this article:

Lv D, Su Y, Li J, Zhu H, Tang Q, Yu Y. Ginkgolide B alleviates renal and podocyte injury in membranous nephropathy by inhibiting ferroptosis. Bangladesh J Pharmacol. 2025; 20: 122-30.

Abstract

This study investigated whether ginkgolide B alleviates renal and podocyte injury in membranous nephropathy by inhibiting ferroptosis. Rats with passive Heymann nephritis received ginkgolide B (7.5 mg/kg/day) or vehicle. Ginkgolide B significantly ameliorated nephrotic syndrome, reducing 24-hour urinary protein excretion, and improving serum albumin levels. It also normalized lipid profiles and enhanced renal function, with all changes achieving statistical significance at $p < 0.05$. Histopathological analysis revealed reduced glomerular immune deposits, preserved podocyte density indicated by improved WT-1 nuclear expression/distribution, and restored slit diaphragm integrity shown by increased CD2AP expression. Mechanistically, ginkgolide B suppressed ferroptosis by significantly decreasing reactive oxygen species and lipid peroxides, reducing iron deposition, downregulating ferroptosis drivers NCOA4, ACSL4, and LPCAT3, and restoring glutathione peroxidase 4 activity ($p < 0.05$ for all). These findings demonstrate that ginkgolide B mitigates membranous nephropathy-associated renal and podocyte injury by inhibiting ferroptosis.

Introduction

Membranous nephropathy is an autoimmune glomerular disease characterized histologically by subepithelial immune deposits along the glomerular basement membrane and clinically by nephrotic-range proteinuria (Ponticelli, 2025). The incidence of membranous nephropathy is increasing worldwide, with longitudinal data indicating a 13% annual increase in China (Xu et al., 2016).

The management of membranous nephropathy relies on non-specific immunosuppression, mainly owing to an incomplete understanding of the pathological mechanisms underlying renal injury. Podocytes represent the primary target of injury in membranous nephropathy, with autoantibodies initiating subepithelial

immune complex formation and complement activation (Kistler and Salant, 2024). Therefore, understanding the mechanisms underlying renal and podocyte damage in membranous nephropathy is necessary for improving the treatment.

Ferroptosis is an iron-dependent form of regulated cell death characterized by accumulation of phospholipid hydroperoxides, which cause plasma membrane rupture through peroxidation of polyunsaturated fatty acids (Alves et al., 2025). Recent studies have suggested the involvement of ferroptosis in podocyte injury in various kidney diseases, such as diabetic kidney disease (Gao et al., 2025; Li et al., 2023; Pei et al., 2025; Zhang et al., 2025), lupus nephritis (Liu et al., 2025), focal segmental glomerulosclerosis (He et al., 2023) and Fabry disease (Wise et al., 2025), highlighting the therapeutic



potential of ferroptosis inhibitors. However, the role of ferroptosis and its inhibitors in membranous nephropathy remains unclear.

Ginkgolide B, a bioactive diterpenoid lactone isolated from *Ginkgo biloba* L. leaves, is a pharmacologically active component with anti-inflammatory, antioxidant, and cytoprotective effects (Ahlemeyer and Kriegelstein, 2003). Notably, emerging evidence indicates that ginkgolide B exerts anti-ferroptotic effects across various pathological contexts. In diabetic kidney disease models, ginkgolide B preserves renal function by inhibiting GPX4 ubiquitination and attenuating lipid peroxidation (Chen et al., 2022). Similarly, in neurological disorders such as cerebral ischemia and spinal cord injury, ginkgolide B mitigates ferroptosis by reducing iron accumulation and oxidative stress (She et al., 2025; Yang et al., 2024). These findings collectively suggest that ferroptosis inhibition represents a conserved therapeutic mechanism of ginkgolide B.

Given the pivotal role of ferroptosis in podocyte injury across diverse kidney diseases and the demonstrated anti-ferroptotic efficacy of ginkgolide B, it is hypothesized that ginkgolide B might alleviate membranous

nephropathy-related renal injury by inhibiting ferroptosis. To test this hypothesis, classical passive Heymann nephritis model of membranous nephropathy was used.

Materials and Methods

Experimental animals

Sprague-Dawley rats (female; 150–180 g) were obtained from SPF Biotechnology Co., Ltd. (China) and housed in the Laboratory Animal Center of Wuxi School of Medicine, Jiangnan University. The rats had *ad libitum* access to water and standard chow.

Grouping, and intervention

Rats were randomly assigned to four groups (n=10/group initially): normal control, ginkgolide B-only, passive Heymann nephritis, and passive Heymann nephritis + ginkgolide B. Ginkgolide B (Aladdin Scientific Corp., China) was administered at a dosage of 7.5 mg/kg/day from the day of model induction until sacrifice.

Box 1: Rat model of passive Heymann nephritis

Principle

The passive Heymann nephritis model represents antibody-mediated experimental glomerulonephritis mimicking human membranous nephropathy. Heterologous antibodies targeting the renal tubular antigen Fx1A bind to glomerular epitopes, forming subepithelial immune deposits. This process induces complement activation, podocyte injury, and proteinuria.

Materials

Animals: Male New Zealand rabbits and Sprague-Dawley rats. Reagents: Fx1A antigen (isolated from Sprague-Dawley rat renal cortex), complete Freund's adjuvant, normal saline, and fluorescein isothiocyanate-conjugated anti-rabbit IgG. Equipment: Sieve mesh (150 mesh), centrifuge, lyophilizer, refrigerator, and fluorescence microscope.

Procedure

Fx1A antigen preparation

Step 1: Isolate the renal cortex from euthanized rats, homogenize, and sieve.

Step 2: Centrifuge the homogenate (4°C, 400 × g, 10 min) and discard precipitate.

Step 3: Ultracentrifuge the supernatant (4°C, 78,680 × g, 45 min), wash pellet in deionized water, lyophilize, and store at –80°C.

Rabbit Anti-Fx1A antiserum production

Step 1: Emulsify 10 mg of Fx1A in 0.5 mL of normal saline with 0.5 mL of complete Freund's adjuvant.

Step 2: Inject the solution subcutaneously at multiple dorsal sites in rabbits.

Step 3: Administer ≥4 booster doses at intervals of 10-20 days.

Step 4: Collect serum 10 days after the final booster, centrifuge (4°C, 1,000 × g, 10 min), and store at –80°C.

Step 5: Inactivate complement (56°C, 30 min) before use.

Antiserum potency validation

Step 1: Add serially diluted (1:1,000–1:4,000) antiserum to normal rat kidney cryosections.

Step 2: Detect binding using fluorescein isothiocyanate-conjugated anti-rabbit IgG (1:100).

Step 3: The validation criterion is bright linear fluorescence along proximal tubular brush borders at ≤1:2,000 dilution.

Passive Heymann nephritis induction

Step 1: Inject 2 mL of anti-Fx1A antiserum intraperitoneally into non-anesthetized rats.

Step 2: Administer 1 mL of antiserum intraperitoneally after 1 hour (total 3 mL/rat).

Exclusion criteria

a) Exclude rats with 24-hours urinary protein excretion of <10 mg on day 15 after Fx1A injection; b) Exclude rats that died during the model induction phase.

This protocol modifies classical methods by using rabbits for antiserum production, enhances the immune process, simplifies potency validation, involves intraperitoneal administration, and includes stringent exclusion criteria to enhance reproducibility and safety.

Reference

Salant and Cybulsky, 1988.

Sample collection

On day 15 after model induction, rats were placed in metabolic cages for 24-hours urine collection. Blood (1.0–1.5 mL) was collected from the angular vein for serum isolation. The kidneys were perfused *in situ* with ice-cold phosphate-buffered saline through the renal artery until blanched, and renal cortex tissue was excised. Rats that died during the observation period or had 24-hours urinary protein of <10 mg were excluded, resulting in the inclusion of 8 rats/group in the final analysis.

Urinary protein and serum biochemical analyses

24-hours urinary protein was quantified using a Bradford protein assay kit (P0006, Beyotime Biotechnology, China). Serum albumin, triglyceride, total cholesterol, low-density lipoprotein cholesterol, high-density lipoprotein cholesterol, creatinine, and blood urea nitrogen levels were measured using an automated biochemical analyzer (ZY-450, Kehua Bioengineering Co., Ltd., China).

Histopathological and immunohistochemical analyses

Masson staining and periodic acid–silver methenamine staining were performed on paraffin-embedded tissue sections (2.5 μ m) using commercial kits (G1006, G1059; Servicebio Technology Co., Ltd., China) according to standardized protocols. For immunohistochemical analysis, the sections were subjected to antigen retrieval in citrate buffer (pH 6.0) under high-pressure heating; blocked with 3% bovine serum albumin; and incubated with primary antibodies against WT-1 (1:100, GB11382, Servicebio), NCOA4 (1:100, DF4255, Affinity Biosciences Ltd., China), ACSL4 (1:50, DF15820, Affinity), and LPCAT3 (1:150, 67882-1-Ig, Proteintech Group, Inc, China) overnight at 4°C. For detection, the sections were treated with horseradish peroxidase–conjugated secondary antibodies (1:200–500, GB23301/GB23303, Servicebio) and stained with 3,3'-diaminobenzidine for color development. For immunofluorescence staining, 5- μ m frozen sections were incubated with anti-CD2AP antibody (1:200, 32089-1-AP, Protein-tech) followed by a fluorescein isothiocyanate–conjugated secondary antibody (1:200, A0562, Beyotime). The sections were stained with prussian blue working solution (G1029, Servicebio) for 1 hour, and nuclei were counterstained with nuclear fast red.

All images were acquired using a Panoramic Pathology Scanner (MIDI, 3DHISTECH Ltd., Hungary) or a confocal microscope (LSM710, Carl Zeiss Meditec AG, Germany). For semiquantitative immunohistochemical analysis, integrated optical density per glomerular area was measured in three randomly selected glomeruli per section using the Image-Pro Plus 6.0 software (Media Cybernetics, USA).

Biochemical assays

Reactive oxygen species levels in rat renal cortex tissues

were quantified through fluorescence spectroscopy (Ex/Em: 488/525 nm) using the 2',7'-dichlorodihydrofluorescein diacetate probe (E004-1-1, Nanjing Jiancheng Bioengineering Institute, China).

Lipid peroxide content was determined on a spectrophotometer at 586 nm using an A106-1-2 assay kit (Jiancheng Bioengineering).

Glutathione peroxidase 4 (GPX4) activity was determined by monitoring the decrease in absorbance at 340 nm caused by the consumption of a reducing agent. Specificity was confirmed using an inhibitor-controlled assay (E-BC-K883-M, Elabscience Biotechnology Co., Ltd., China).

Statistical analysis

Data were expressed as the mean \pm standard deviation. Intergroup differences were analyzed using one-way analysis of variance with post-hoc least significant difference test (equal variance) or Welch's analysis of variance with Dunnett's T3 test (unequal variance) in the Statistical Package for the Social Sciences (version 22.0) software (IBM Corp., USA). Statistical significance was defined as a p-value of <0.05 (two-tailed).

Results

Effects on nephrotic syndrome

Compared with rats in the normal control groups, those in the passive Heymann nephritis group developed classic features of nephrotic syndrome, including severe proteinuria (Figure 1A); hypoalbuminemia (Figure 1B), dyslipidemia characterized by elevated triglyceride, total cholesterol, low-density lipoprotein cholesterol, and high-density lipoprotein cholesterol levels (Figures 1C–F), and impaired renal function characterized by increased serum creatinine and blood urea nitrogen levels (Figures 1G–H).

Ginkgolide B treatment ameliorated these manifestations, significantly reducing 24-hours urinary protein levels (Figure 1A), restoring serum albumin levels (Figure 1B), normalizing lipid profiles (Figures 1C–F), and improving renal function (Figures 1G–H). No significant differences were found in 24-hours urinary protein levels, serum albumin levels, lipid profiles, or renal function between the normal control and ginkgolide B-only groups (Figures 1A–H), validating the safety of ginkgolide B. These results collectively suggest that ginkgolide B can alleviate nephrotic syndrome in rat models of passive Heymann nephritis.

Effects on renal and podocyte injury

Rats in the passive Heymann nephritis group exhibited hallmark pathological features of membranous nephropathy. Masson staining showed subepithelial eosino-

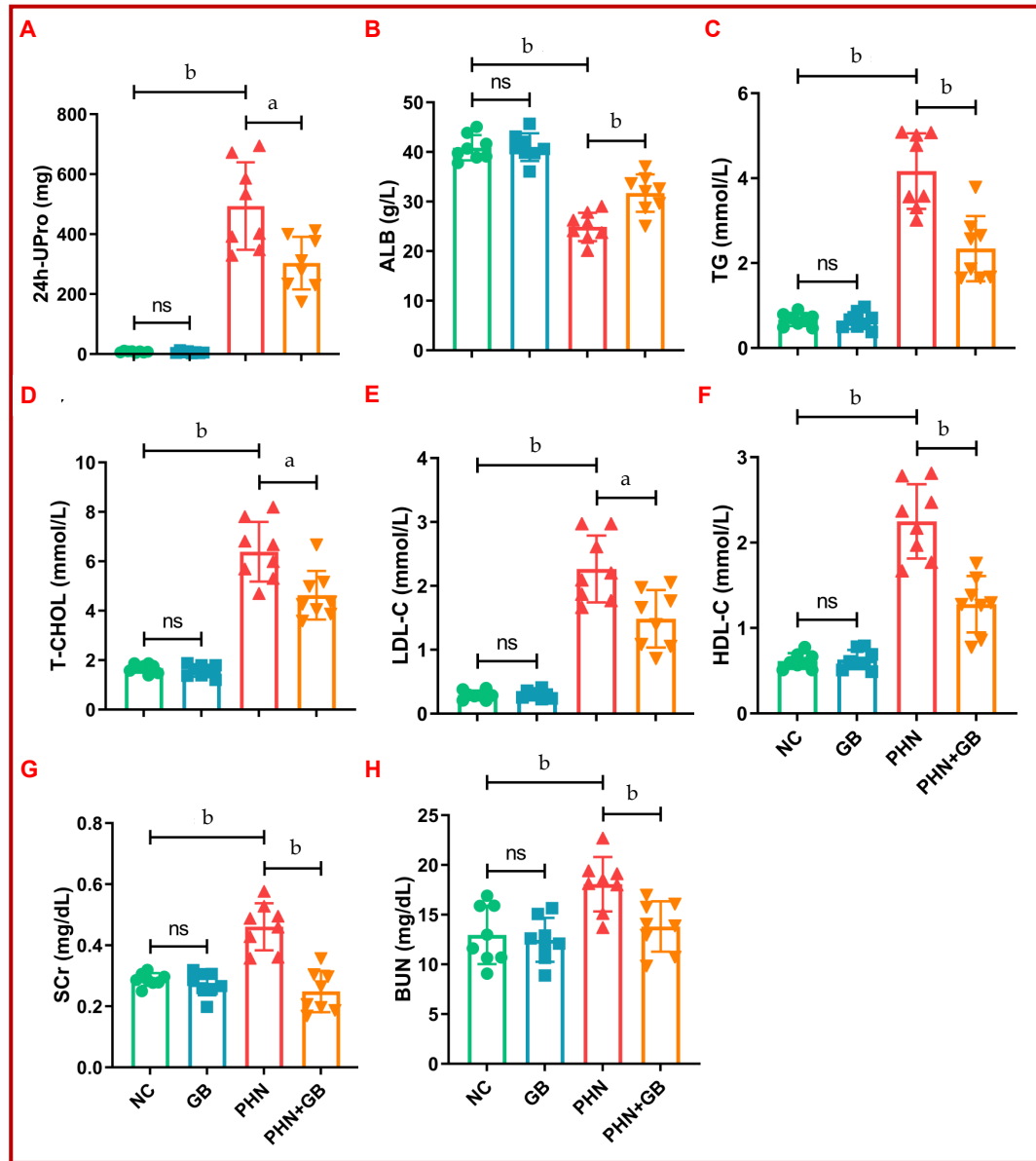


Figure 1: Effects of ginkgolide B on nephrotic syndrome in rats with passive Heymann nephritis. 24-hours urinary protein (24h-UPro) (A), serum albumin (ALB) (B), triglyceride (TG) (C), total cholesterol (T-CHOL) (D), low-density lipoprotein cholesterol (LDL-C) (E), high-density lipoprotein cholesterol (HDL-C) (F), serum creatinine (SCr) (G), and blood urea nitrogen (BUN) (H) levels in rats from different groups (n = 8/group). Data are expressed as the mean \pm standard deviation. ns, no significance; ^ap<0.05; ^bp<0.01; NC (normal control), GB (ginkgolide B-only), PHN (passive Heymann nephritis), and PHN + GB (PHN with GB treatment)

philic deposits, indicating accumulation of immune complexes along the glomerular basement membrane. Periodic acid-silver methenamine staining showed characteristic spike-like projections, indicating reactive basement membrane hyperplasia. WT-1 expression in podocyte nuclei was markedly decreased and irregularly distributed, indicating podocyte injury and loss. Immunofluorescence staining showed discontinuous distribution and reduced expression of the slit diaphragm protein CD2AP, indicating disrupted structural integrity of podocytes (Figure 2).

Ginkgolide B treatment attenuated these pathological changes, reducing immune deposits to some extent, diminishing periodic acid-silver methenamine-positive spikes, preserving podocyte density, and improving CD2AP expression and continuity. No significant pathological changes were observed in the normal control or ginkgolide B-only group (Figure 2). These findings suggest that ginkgolide B can mitigate renal and podocyte injury in rat models of passive Heymann nephritis.

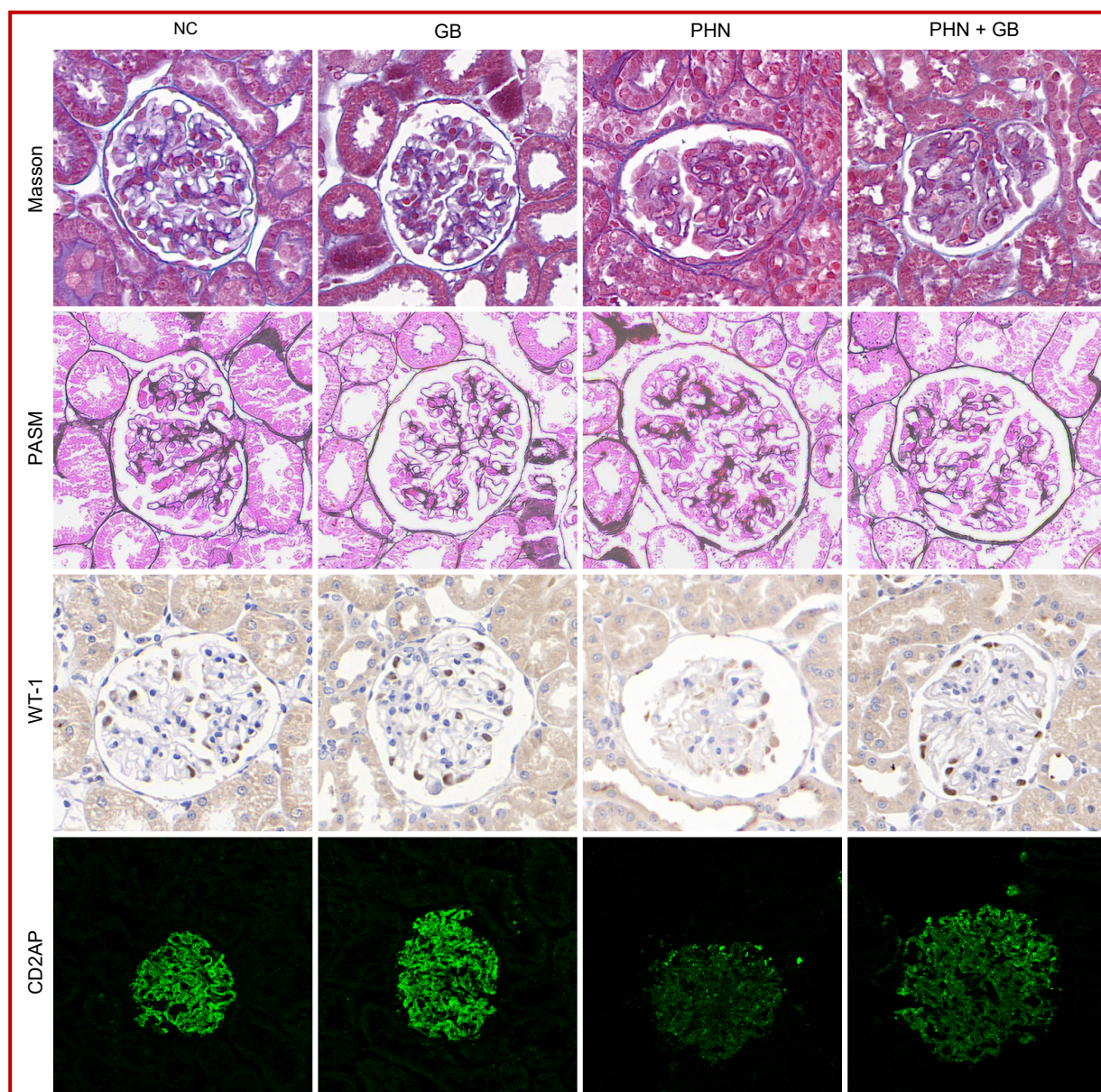


Figure 2: Effects of ginkgolide B on renal and podocyte injury in rats with passive Heymann nephritis. Representative images of Masson staining, periodic acid–silver methenamine (PASM) staining, WT-1 immunohistochemical staining and CD2AP immunofluorescence staining in rat renal tissues from different groups (n=8/group). NC (normal control), GB (ginkgolide B-only), PHN (passive Heymann nephritis), and PHN + GB (PHN with GB treatment). Original magnification: $\times 400$ (CD2AP), $\times 630$ (Masson, PASM, and WT-1)

Effects on renal ferroptosis

Ferroptosis activation was observed in the kidneys of rats with passive Heymann nephritis. In particular, reactive oxygen species levels were markedly elevated (Figure 3A), indicating increased oxidative stress, a key driver of ferroptosis. Concurrently, lipid peroxide accumulation validated extensive peroxidation of polyunsaturated fatty acids (Figure 3B), a hallmark of ferroptosis-induced membrane damage. Prussian blue staining showed pronounced iron deposition in glomeruli (Figure 3G), indicating iron overload critical for ferroptosis execution. Immunohistochemical analysis demon-

strated upregulation of ferroptosis-promoting factors, including NCOA4, ACSL4, and LPCAT3 (Figures 3C–E, G), and suppressed activity of the ferroptosis-inhibiting enzyme GPX4 (Figure 3F).

Ginkgolide B treatment effectively reversed these changes, reducing reactive oxygen species and lipid peroxide levels, diminishing iron deposition, down-regulating ferroptosis-promoting factors, and restoring GPX4 activity (Figures 3A–G). No ferroptosis-related changes were observed in the normal control or ginkgolide B-only group (Figures 3A–G). Altogether, these results indicate that ginkgolide B alleviates renal

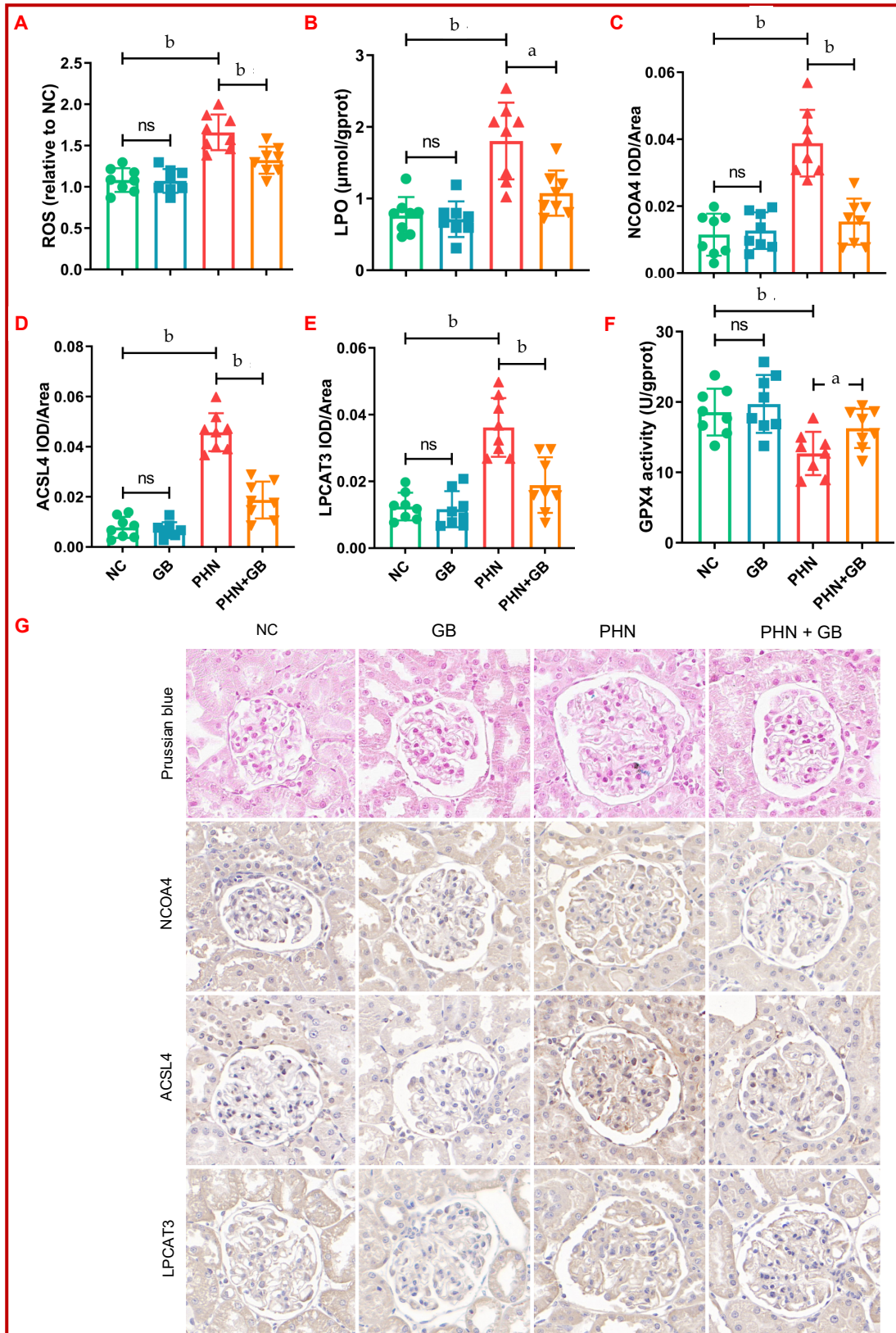


Figure 3: Effects of ginkgolide B on renal ferroptosis in rats with passive Heymann nephritis. Reactive oxygen species (ROS) levels (A), lipid peroxide (LPO) levels (B), immunohistochemical semiquantitative analysis of NCOA4 (C), ACSL4 (D), LPCAT3 (E), and GPX4 activity (F), and representative images of Prussian blue staining and immunohistochemical staining for NCOA4, ACSL4, and LPCAT3 (G) in rat renal tissues from different groups (n=8/group). NC (normal control), GB (ginkgolide B-only), PHN (passive Heymann nephritis), and PHN + GB (PHN with GB treatment). Data are mean \pm standard deviation. ns, no significance; ^ap<0.05; ^bp<0.01. Original magnification: $\times 630$

ferroptosis in rat models of passive Heymann nephritis.

Discussion

This study establishes ferroptosis as a pathogenic mechanism in membranous nephropathy and proposes ginkgolide B as an inhibitor of this mechanism. The coordinated dysregulation of ferroptosis biomarkers, including reactive oxygen species/lipid peroxide accumulation, iron overload, upregulation of NCOA4/ACSL4/LPCAT3, and GPX4 suppression, collectively indicated ferroptosis activation in the kidneys of rats with passive Heymann nephritis. Mechanistically, reactive oxygen species elevation catalyzes the oxidation of polyunsaturated fatty acids in membrane phospholipids, initiating a peroxidation cascade that directly ruptures plasma membranes. Lipid peroxide accumulation indicates peroxidation of polyunsaturated fatty acid-phospholipids, leading to membrane integrity disruption and osmotic cell rupture. Upregulation of NCOA4 promotes ferritinophagy, resulting in the release of labile iron to fuel Fenton reactions that amplify lipid peroxidation. Upregulation of ACSL4 activates peroxidation-susceptible long-chain polyunsaturated fatty acids and incorporates them into membrane phospholipids. Overexpression of LPCAT3 remodels membranes by inserting polyunsaturated fatty acid-phospholipids, thereby accelerating peroxidation-driven membrane damage. Inactivation of GPX4 disrupts the primary defense against phospholipid hydroperoxides, resulting in peroxide accumulation (Dixon and Olzmann, 2024). These alterations collectively define the iron-dependent, lipid peroxidation-driven cell death pathway characteristic of ferroptosis.

Our findings suggest that ferroptosis drives renal and podocyte injury in membranous nephropathy, which is consistent with the findings of studies that have shown ferroptosis as a common pathogenic mechanism in various podocyte-associated kidney diseases. In diabetic kidney disease, hyperglycemia and advanced glycation end products induce podocyte ferroptosis through inhibition of Nrf2 (Gao et al., 2025), suppression of AMPK (J. Zhang et al., 2025), or dysregulation of the p53/GPX4 axis (Pei et al., 2025), which contrasts with the immune complex-driven pathological changes in membranous nephropathy. In lupus nephritis, autoimmune-driven oxidative stress activates ferroptosis, which can be mitigated by restoring Nrf2/HO-1/GPX4 pathway activity (Liu et al., 2025). This phenomenon is consistent with antioxidant dysfunction observed in rat models of passive Heymann nephritis in this study. Ferroptosis also contributes to focal segmental glomerulosclerosis, where GPX4 downregulation in podocytes was reversed by ferroptosis inhibitor ferrostatin-1, attenuating proteinuria and fibrosis (He et al., 2023); though triggered by adriamycin rather than immune

complexes and complement as in membranous nephropathy, both conditions converge on ferroptosis-driven podocyte injury. Genetic disorders such as Fabry disease exhibit ferroptosis owing to sphingolipid accumulation, which upregulates ALOX15 in podocytes (Wise et al., 2025), whereas membranous nephropathy may involve acquired iron dysmetabolism. All of the abovementioned podocyte injuries lead to activation of ferroptosis through lipid peroxidation, iron dependency, or antioxidant impairment. In addition to its role in podocytopathies such as membranous nephropathy, ferroptosis contributes to tubular injury and other glomerular diseases, such as unilateral ureteral obstruction-induced fibrosis (Huang et al., 2025), cisplatin-induced acute kidney injury (Zheng et al., 2025), adenine-induced chronic kidney disease (Fu et al., 2025; Kim et al., 2025), aging kidneys (Wang et al., 2025), crystal nephropathy, and IgA nephropathy (Qing et al., 2025; Tang et al., 2025). This universal involvement of ferroptosis indicates its important role in renal injury across kidney diseases, highlighting the therapeutic potential of ferroptosis inhibitors.

This study suggests that ginkgolide B exerts renoprotective effects in membranous nephropathy through multi-targeted suppression of ferroptosis. The therapeutic efficacy of ginkgolide B may result from its coordinated intervention at critical regulatory nodes: it suppresses the initial trigger by mitigating iron overload, attenuates the propagating oxidative stress, and prevents ferroptosis execution by inhibiting lipid peroxidation. Concurrently, ginkgolide B regulates the molecular network driving ferroptosis, normalizing the levels of both pro-ferroptotic and anti-ferroptotic factors. This coordinated modulation synergistically disrupts the self-amplifying cycle of iron-dependent phospholipid peroxidation, distinguishing the action of ginkgolide B from that of single-pathway inhibitors and highlighting its potent functional and structural protection in passive Heymann nephritis. The inhibition of ferroptosis by ginkgolide B represents a conserved therapeutic mechanism across diseases. In cerebral ischemia and spinal cord injury, ginkgolide B mitigates neuronal damage by reducing iron accumulation, reactive oxygen species levels, and lipid peroxide levels, mirroring its suppression of iron overload, oxidative stress, and membrane peroxidation in membranous nephropathy (She et al., 2025; Yang et al., 2024). In Alzheimer's disease and nonalcoholic fatty liver disease, ginkgolide B inhibits ferroptosis drivers, validating its core capacity to disrupt the ferroptosis cascade (Shao et al., 2021; Yang et al., 2020; Y. Zhang et al., 2023). These anti-ferroptotic effects extend the cytoprotective effect of ginkgolide B, highlighting its promise as a broad-spectrum inhibitor of ferroptosis. Furthermore, clinical safety evaluations have consistently reported fewer adverse events of ginkgolide B in various diseases, including ischemic stroke and severe

sepsis (Dhainaut et al., 1994; Zhao et al., 2022). These findings align with our observation of no significant adverse effects in ginkgolide B-treated rats. Therefore, ginkgolide B may be a safe and effective ferroptosis inhibitor with high therapeutic potential for membranous nephropathy.

Despite notable findings, this study has some limitations. Although we identified ferroptosis as a target of ginkgolide B in membranous nephropathy, potential crosstalk with other pathways remains unclear. In addition, therapeutic outcomes were assessed only at a single time point, precluding the evaluation of long-term efficacy and safety.

Conclusion

Ferroptosis leads to renal and podocyte injury in membranous nephropathy. Ginkgolide B effectively attenuates this injury by inhibiting ferroptosis, serving as a promising therapeutic agent for membranous nephropathy.

Financial Support

This study was supported by the Wuxi Municipal Science and Technology Development Fund (Taihu Light Science and Technology Research Project, Grant No. K20241017), the Scientific Research Program of the Wuxi Commission of Health (Q202308), the Wuxi Aging Research Project (WXLN25-B-04), and the Joint Clinical Medicine and Management Research Project for Regional Medical Center Construction under the Pairing Assistance Program between Affiliated Hospital of Jiangnan University and Donghai County People's Hospital.

Ethical Issue

All animal experiments were reviewed and approved by the Experimental Animal Ethics Committee of Jiangnan University (JN. No. 20250515S0300801/275).

Conflict of Interest

Authors declare no conflict of interest

References

- Ahlemeyer B, Kriegelstein J. Pharmacological studies supporting the therapeutic use of *Ginkgo biloba* extract for Alzheimer's disease. *Pharmacopsychiatry*. 2003; 36 Suppl 1: S8-14.
- Alves F, Lane D, Nguyen TPM, Bush AI, Ayton S. In defence of ferroptosis. *Signal Transduct Target Ther*. 2025; 10: 2.
- Chen J, Ou Z, Gao T, Yang Y, Shu A, Xu H, Chen Y, Lv Z. Ginkgolide B alleviates oxidative stress and ferroptosis by inhibiting GPX4 ubiquitination to improve diabetic nephropathy. *Biomed Pharmacother*. 2022; 156: 113953.
- Dhainaut JF, Tenaillon A, Le Tulzo Y, Schlemmer B, Solet JP, Wolff M, Holzapfel L, Zeni F, Dreyfuss D, Mira JP, Vathaire F, Guinot P. Platelet-activating factor receptor antagonist BN 52021 in the treatment of severe sepsis: A randomized, double-blind, placebo-controlled, multicenter clinical trial. *BN 52021 Sepsis Study Group. Crit Care Med*. 1994; 22: 1720-28.
- Dixon SJ, Olzmann JA. The cell biology of ferroptosis. *Nat Rev Mol Cell Biol*. 2024; 25: 424-42.
- Fu W, Zhang M, Meng Y, Wang J, Sun L. Increased NPM1 inhibit ferroptosis and aggravate renal fibrosis via Nrf2 pathway in chronic kidney disease. *Biochim Biophys Acta Mol Basis Dis*. 2025; 1871: 167551.
- Gao K, Liu Y, Li K, Liu L, Cai Y, Zhang X, Zhao Z. Nrf2-mediated ferroptosis is involved in Berberine-induced alleviation of diabetic kidney disease. *Phytother Res*. 2025.
- He X, Yang L, Wang M, Zhang P, Wang R, Ji D, Gao C, Xia Z. Targeting ferroptosis attenuates podocytes injury and delays tubulointerstitial fibrosis in focal segmental glomerulosclerosis. *Biochem Biophys Res Commun*. 2023; 678: 11-16.
- Huang Z, Zhou L, Liu B, Li X, Sang Y. Endoplasmic reticulum stress aggravates ferroptosis via PERK/ATF4/HSPA5 pathway in UUO-induced renal fibrosis. *Front Pharmacol*. 2025; 16: 1545972.
- Kim JM, Kim Y, Na HJ, Hur HJ, Lee SH, Sung MJ. *Magnolia kobus* DC. Alleviates adenine-induced chronic kidney disease by regulating ferroptosis in C57BL/6 mice. *Front Pharmacol*. 2025; 16: 1548660.
- Kistler AD, Salant DJ. Complement activation and effector pathways in membranous nephropathy. *Kidney Int*. 2024; 105: 473-83.
- Li L, Dai Y, Ke D, Liu J, Chen P, Wei D, Wang T, Teng Y, Yuan X, Zhang Z. Ferroptosis: new insight into the mechanisms of diabetic nephropathy and retinopathy. *Front Endocrinol (Lausanne)*. 2023; 14: 1215292.
- Liu C, Liu X, Wang Y, Yu H, Li Q, Zheng Y, Fu Y, Yao G, Sun L. Mesenchymal stromal cells reduce ferroptosis of podocytes by activating the Nrf2/HO-1/GPX4 pathway in lupus nephritis. *Int Immunopharmacol*. 2025; 153: 114537.
- Pei Z, Chen Y, Zhang Y, Zhang S, Wen Z, Chang R, Ni B, Ni Q. Hirsutine mitigates ferroptosis in podocytes of diabetic kidney disease by downregulating the p53/GPX4 signaling pathway. *Eur J Pharmacol*. 2025; 991: 177289.
- Ponticelli C. Membranous nephropathy. *J Clin Med*. 2025; 14.
- Qing J, Zhang L, Fan R, Zhi H, Li C, Li Y, Wu J, Han C, Li Y. GPX4 expression changes in proximal tubule cells highlight the role of ferroptosis in IgAN. *Sci Rep*. 2025; 15: 3886.
- Salant DJ, Cybulsky AV. Experimental glomerulonephritis. *Methods Enzymol*. 1988; 162: 421-61.
- Shao L, Dong C, Geng D, He Q, Shi Y. Ginkgolide B protects against cognitive impairment in senescence-accelerated P8 mice by mitigating oxidative stress, inflammation and ferroptosis. *Biochem Biophys Res Commun*. 2021; 572: 7-14.

- She W, Ma W, Zhang T, Wu X, Li J, Li X. Ginkgolide B inhibits ferroptosis in PC12 cells and ameliorates the oxidative stress in spinal cord injury through activating Nrf2 signaling pathway. *J Pharmacol Sci.* 2025; 158: 199-206.
- Tang K, Ye T, He Y, Ba X, Xia D, Peng E, Chen Z, Ye Z, Yang X. Ferroptosis, necroptosis, and pyroptosis in calcium oxalate crystal-induced kidney injury. *Biochim Biophys Acta Mol Basis Dis.* 2025; 1871: 167791.
- Wang Z, Dai Y, Jin R, Mo D, Hu Q, Huang Y, Zhang L, Zhang C, Gao H, Yan Q. Ferroptosis activation contributes to kidney aging in mice by promoting tubular cell senescence. *J Gerontol A Biol Sci Med Sci.* 2025; 80.
- Wise AF, Krisnadevi IA, Bruell S, Lee HC, Bhuvan T, Kassianos AJ, Saini S, Wang X, Healy HG, Qian EL, Elliot DA, Steele JR, Fuller M, Nicholls KM, Ricardo SD. Fabry disease podocytes reveal ferroptosis as a potential regulator of cell pathology. *Kidney Int Rep.* 2025; 10: 535-48.
- Xu X, Wang G, Chen N, Lu T, Nie S, Xu G, Zhang P, Luo Y, Wang Y, Wang X, Schwartz J, Geng J, Hou FF. Long-term exposure to air pollution and increased risk of membranous nephropathy in China. *J Am Soc Nephrol.* 2016; 27: 3739-46.
- Yang Y, Chen J, Gao Q, Shan X, Wang J, Lv Z. Study on the attenuated effect of ginkgolide B on ferroptosis in high fat diet induced nonalcoholic fatty liver disease. *Toxicology* 2020; 445: 152599.
- Yang Y, Wu Q, Shan X, Zhou H, Wang J, Hu Y, Chen J, Lv Z. Ginkgolide B attenuates cerebral ischemia-reperfusion injury via inhibition of ferroptosis through disrupting NCOA4-FTH1 interaction. *J Ethnopharmacol.* 2024; 318: 116982.
- Zhang J, Wu Q, Xia C, Zheng H, Jiang W, Wang Y, Sun W. Qing-Re-Xiao-Zheng-(Yi-Qi) formula attenuates the renal podocyte ferroptosis in diabetic kidney disease through AMPK pathway. *J Ethnopharmacol.* 2025: 120157.
- Zhang Y, Zhao Y, Zhang J, Gao Y, Li S, Chang C, Yang G. Quantitative proteomics reveals neuroprotective mechanism of ginkgolide B in A β (1-42)-induced N2a neuroblastoma cells. *J Integr Neurosci.* 2023; 22: 33.
- Zhao H, Guo Q, Li B, Shi M. The efficacy and safety of Ginkgo terpene lactone preparations in the treatment of ischemic stroke: A systematic review and meta-analysis of randomized clinical trials. *Front Pharmacol.* 2022; 13: 821937.
- Zheng F, Lei JZ, Wang JX, Xu XY, Zhou B, Ge R, Dai M, Dong HK, Wu N, Li YH, Zhu GQ, Zhou YB. Crucial roles of asprosin in cisplatin-induced ferroptosis and acute kidney injury. *Free Radic Biol Med.* 2025; 227: 296-311.

Author Info

Yafen Yu (Principal contact)
e-mail: yafeny@163.com